

Lipopolysaccharides induced inflammatory responses and electrophysiological dysfunctions in human-induced pluripotent stem cell derived cardiomyocytes

Gökhan Yücel^{1,2*}, Zhihan Zhao^{1,2*}, Ibrahim El-Battrawy^{1,2}, Huan Lan^{1,6}, Siegfried Lang^{1,2}, Xin Li¹, Fanis Buljubasic^{1,2}, Wolfram-Hubertus Zimmermann^{3,2}, Lukas Cyganek^{2,7}, Jochen Utikal^{4,2}, Ursula Ravens⁸, Thomas Wieland^{5,2}, Martin Borggrefe^{1,2}, Xiao-Bo Zhou^{1,2,6}, Ibrahim Akin^{1,2}

¹First Department of Medicine, Faculty of Medicine, University Medical Centre Mannheim (UMM), University of Heidelberg, Mannheim, Germany

²DZHK (German Center for Cardiovascular Research), Partner Sites, Heidelberg-Mannheim and Göttingen, Germany

³Institute of Pharmacology and Toxicology, University of Göttingen, Göttingen, Germany

⁴Skin Cancer Unit, German Cancer Research Center (DKFZ), Heidelberg and Department of Dermatology, Venereology and Allergology, University Medical Center Mannheim, University of Heidelberg, Mannheim, Germany;

⁵Institute of Experimental and Clinical Pharmacology and Toxicology, Medical Faculty Mannheim, University of Heidelberg, Mannheim, Germany

⁶Key Laboratory of Medical Electrophysiology of Ministry of Education, Institute of Cardiovascular Research, Southwest Medical University, Luzhou, Sichuan, China

⁷Stem Cell Unit, Heart Research Center Göttingen, Göttingen, Germany

⁸Institute of Experimental Cardiovascular Medicine, University Heart Centre Freiburg•Bad Krozingen, Freiburg, Germany

*equally contributed

Address for correspondence:

Xiao-Bo Zhou, MD

First Department of Medicine

University Medical Centre Mannheim

Theodor-Kutzer-Ufer 1-3

68167 Mannheim

Germany

E-mail: Xiaobo.zhou@medma.uni-heidelberg.de

Legends for supplemental data

Table S1. List of genes, RefSeq numbers and primers for qPCR.

Figure S1. Effects of LPS on IL-6 signaling. **A**, IL-6 concentration in supernatants of hiPSC-CM, which was significantly increased after LPS-treatment in different concentrations for 6h (white bar) or 48h (gray bar) (one-way ANOVA: 6h, $p < 0.0001$; 48h, $p < 0.0001$). **B**, Representative recordings of cardiac TNNT (Tnnt2) and CD126 from FACS-analysis of hiPSC-CM. The positive signal for cardiac Tnnt2 was detected (P2 gate). But there was no specific antibody binding leading to fluorescence signal for CD126 (P3 gate), either with or without LPS-treatment, suggesting that there was no expression of CD 126 in hiPS-CMs. **C**, sCD130 (glycoprotein 130) concentration in supernatants of hiPSC-CM after LPS treatment in different concentrations for 6h (white bar) or 48h (gray bar). Although 6h-treatment had no influence on sCD130 concentration, 48h-treatment with LPS in high concentrations raised sCD130 concentrations (one-way ANOVA: 6h, $p = 0,51$; 48h, $p = 0,019$).

Figure S2. Immunostaining of hiPSC-CM for cardiac structure proteins and NFkb. Nuclear staining was induced with DAPI (blue). **A-B**, FITC-conjugated cTNNT2 antibody at day 30 after differentiation (green). **C**, FITC-conjugated cTNNT2 antibody (green) plus cy5-conjugated titin antibody (red). **D**, FITC-conjugated NFkb-p65 subunit antibody (green) after cardiomyocyte treatment with 10 μ g/ml LPS for 6 hours, showing the nuclear-near signal.

Figure S3. Effect of LPS on apamin-sensitive currents. Membrane currents were recorded in cells treated by either vehicle (A-C) or 1 μ g/ml LPS (D-F) for 48h. **A** and **D**, Representative traces of membrane currents from -80 to +80 mV in absence of apamin. **B** and **E**, Representative traces of membrane currents from -80 to +80 mV in presence of 100 nM apamin. **C** and **F**, Representative traces of apamin-sensitive currents.

Figure S4. Effect of LPS on NS8593-sensitive currents. Membrane currents were recorded in cells treated by either vehicle (A-C) or 1 μ g/ml LPS (D-F) for 48h. **A** and **D**, Representative traces of membrane currents in absence of NS8593. **B** and **E**, Representative traces of membrane currents in presence of 10 μ M NS8593. **C** and **F**, Representative traces of NS8593-sensitive currents.

Figure S5. Effect of LPS on transient outward currents (I_{to}) and L-type Ca^{2+} channel currents (I_{Ca-L}). I_{to} and I_{Ca-L} were evoked by the indicated protocol (B and D) in absence (control) and presence

of LPS. 4-aminopyridine (4-AP, 5mM) was used to isolate I_{to} from other currents. **A**, Mean values of I_{to} at +80 mV. **B**, Representative I_{to} . **C**, Mean values of I_{Ca-L} at 5 mV. **D**, Representative I_{Ca-L} . Values given are mean \pm SEM. n, number of cells. * $p < 0.05$

Figure S6. Effect of LPS on rapidly delayed rectifier currents (I_{Kr}) and slowly delayed rectifier currents (I_{Ks}). I_{Kr} and I_{Ks} were evoked by the indicated protocol (B) in absence (control) and presence of LPS. E-4031 (1 μ M) was used to isolate I_{Kr} and chromanol 293B (10 μ M) was used to isolate I_{Ks} from other currents. **A**, Mean values of I_{Kr} at +40 mV. **B**, Representative traces of I_{Kr} at 40 mV. **C**, Mean values of I_{Ks} at 40 mV. **D**, Representative I_{Ks} at 40 mV. Values given are mean \pm SEM. n, number of cells.

Figure S7. Effect of LPS on pH- and ATP-sensitive currents (I_{KATP}). **A**, I-V curves of alkaline (pH-8) inhibited currents in absence (control) and presence of LPS. **B**, I-V curves of acidosis (pH-6) inhibited currents in absence (control) and presence of LPS. **C**, Mean values of the pH-sensitive currents at 40 mV. **D**, I-V curves in absence and presence of either glybenclamide or nicorandil in control cells. **E**, I-V curves in absence and presence of either glybenclamide or nicorandil in LPS-treated cells. **F**, Mean values of the currents at -70 mV. Values given are mean \pm SEM. n, number of cells.

Figure S8. Effects of LPS on intracellular Ca^{2+} -concentration. **A** and **B**, Representative traces of Ca^{2+} -transients in control and LPS-treated cells. **C** and **D**, Mean values of diastolic and systolic Ca^{2+} -concentration in control and LPS-treated cells. Values given are mean \pm SEM. n, number of cells.

Table S1. List of genes, RefSeq numbers and primers for qPCR.

Gene symbol	RefSeq No.	Cat. No. Primers
ABCC8 (KATP, beta-subunit SUR1)	NM_000352	PPH00038F
CACNA1C (L-type Ca ²⁺ channel)	NM_000719	PPH01378G
CCL5	NM_002985	PPH00703B
CD-14	NM_000591	PPH05723A
GAPDH	NM_002046	PPH00150F
IL1B (IL-1 beta)	NM_000576	PPH00171C
IL6	NM_000600	PPH00560C
IL8	NM_000584	PPH00568A
IL10	NM_000572	PPH00572C
KCND3 (Ito, Kv4.3)	NM_004980	PPH06923A
KCNH2 (IKr, Kv11.1)	NM_000238	PPH01660A
KCNJ11 (K _{ATP} , alpha-subunit)	NM_000525	PPH01409B
KCNK3 (TASK-1)	NM_002246	PPH08513A
KCNN2 (SK2)	NM_021614	PPH01665A
KCNN4 (SK4)	NM_002250	PPH01418C
KCNQ1 (I _{Ks} , Kv7.1)	NM_000218	PPH01419A
LBP	NM_004139	PPH01424F
Ly96 (MD2)	NM_015364	PPH06052A
MCP-1	NM_002982	PPH00192F
NfkappaB1	NM_003998	PPH00204F
RelA	NM_021975	PPH01812B
SCN10A (Na ⁺ channel, Nav1.8)	NM_006514	PPH15064A
SCN5A (Na ⁺ channel, Nav1.5)	NM_000335	PPH01671F
SLC8A1 (NCX1)	NM_021097	PPH12509B
TIRAP	NM_001039661	PPH06246B
TLR4	NM_138554	PPH01795F
TNF-alpha	NM_000594	PPH00341F

RefSeq No. : GenBank NCBI Reference Sequences

Cat. No. Primers: Qiagen RT² qPCR Primer Assays

Figure S1

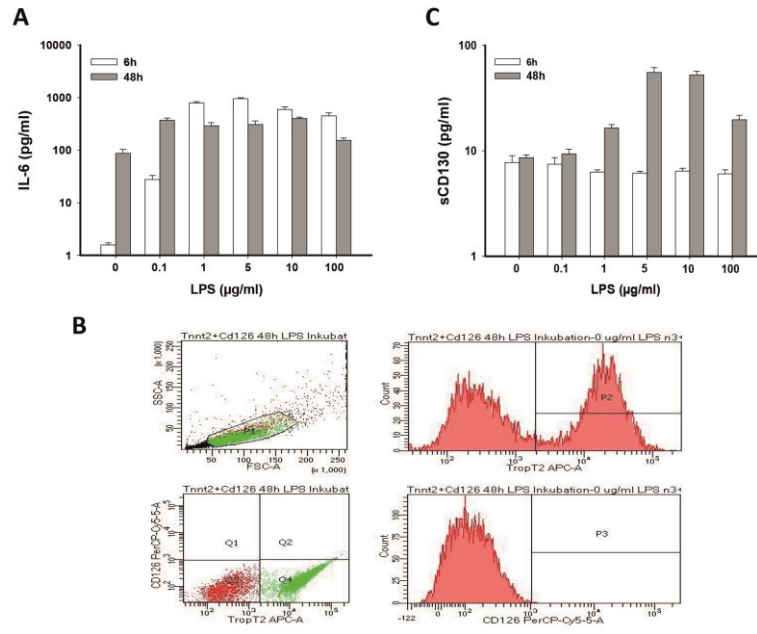


Figure S2

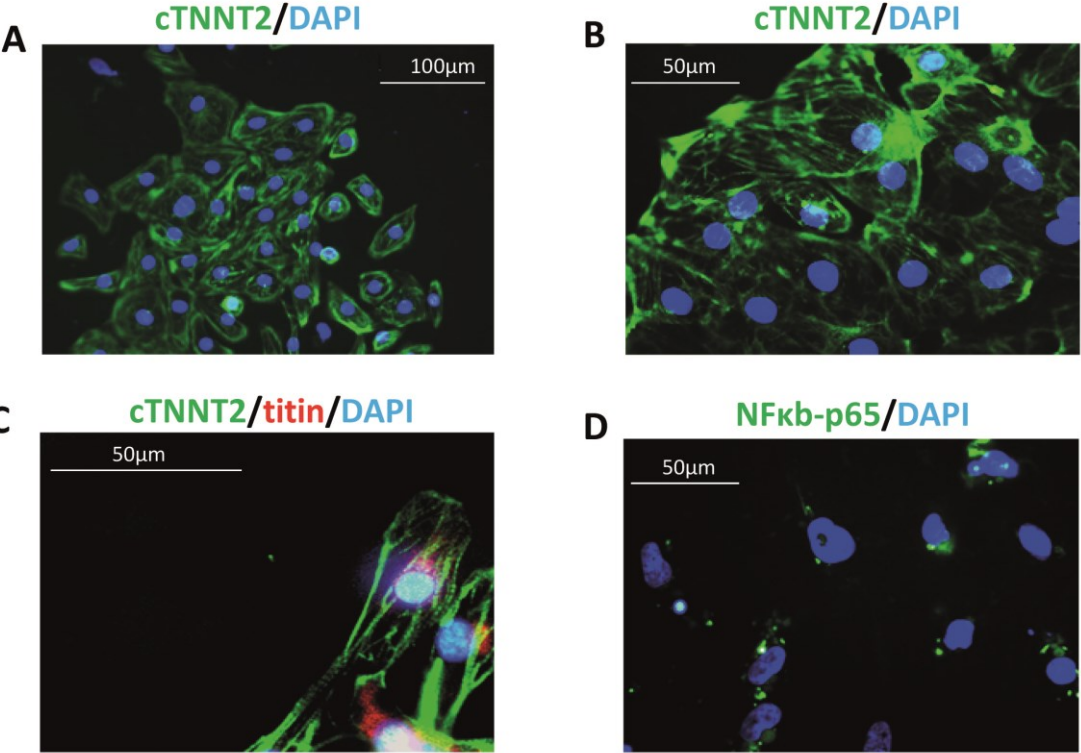


Figure S3

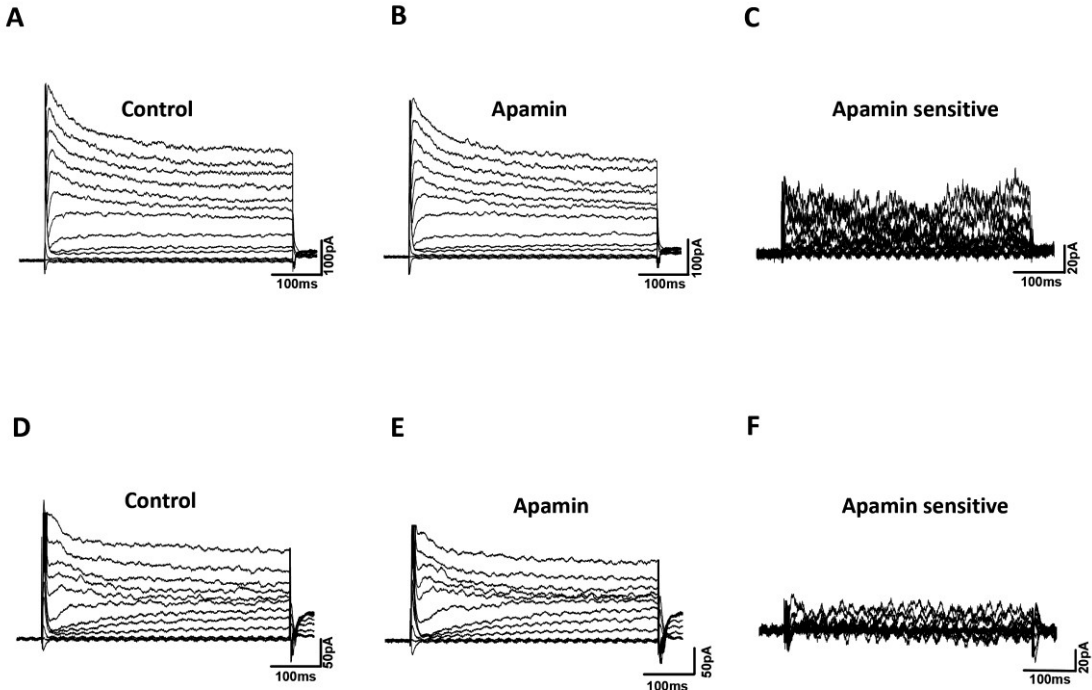


Figure S4

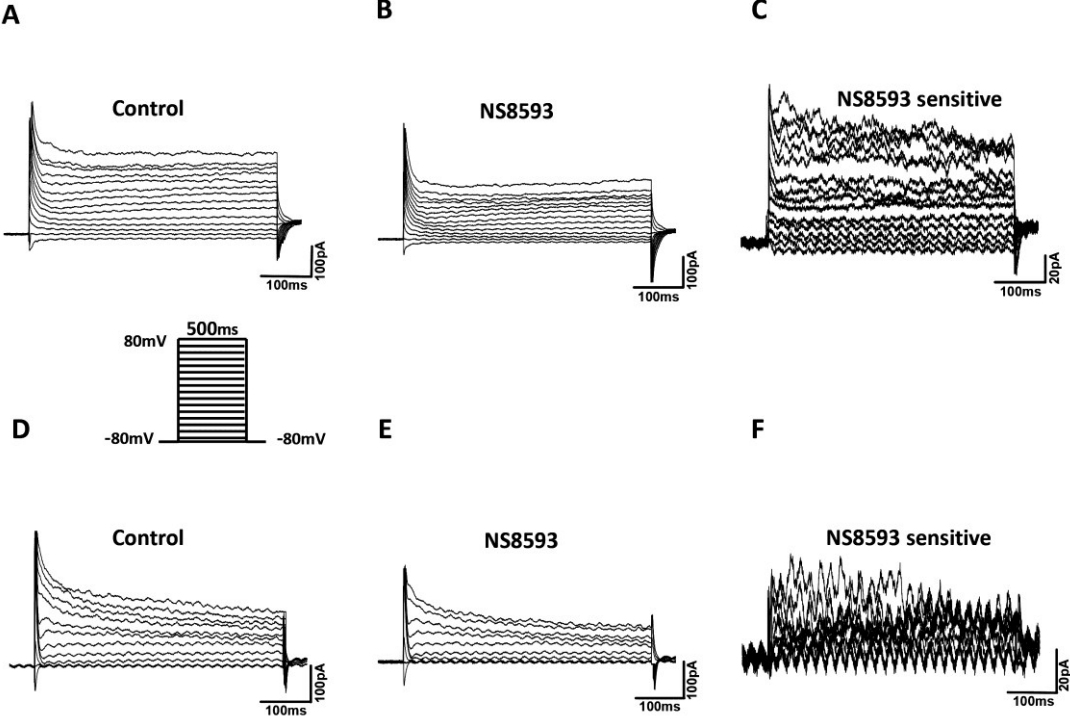


Figure S5

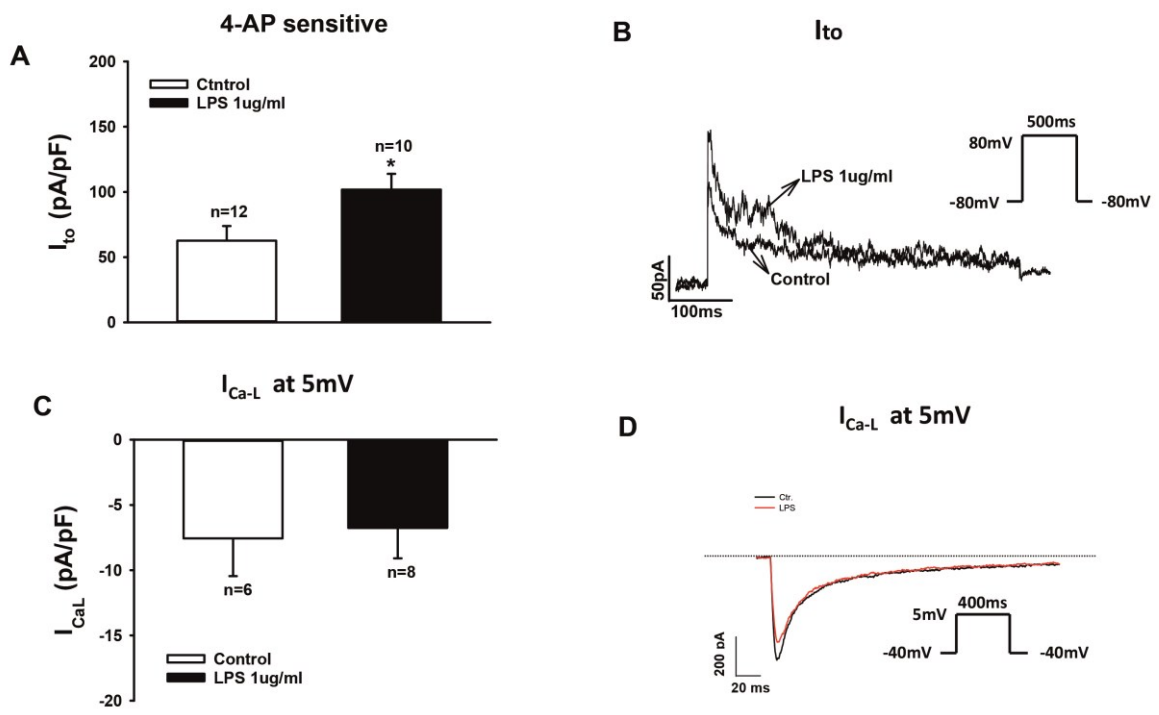


Figure S6

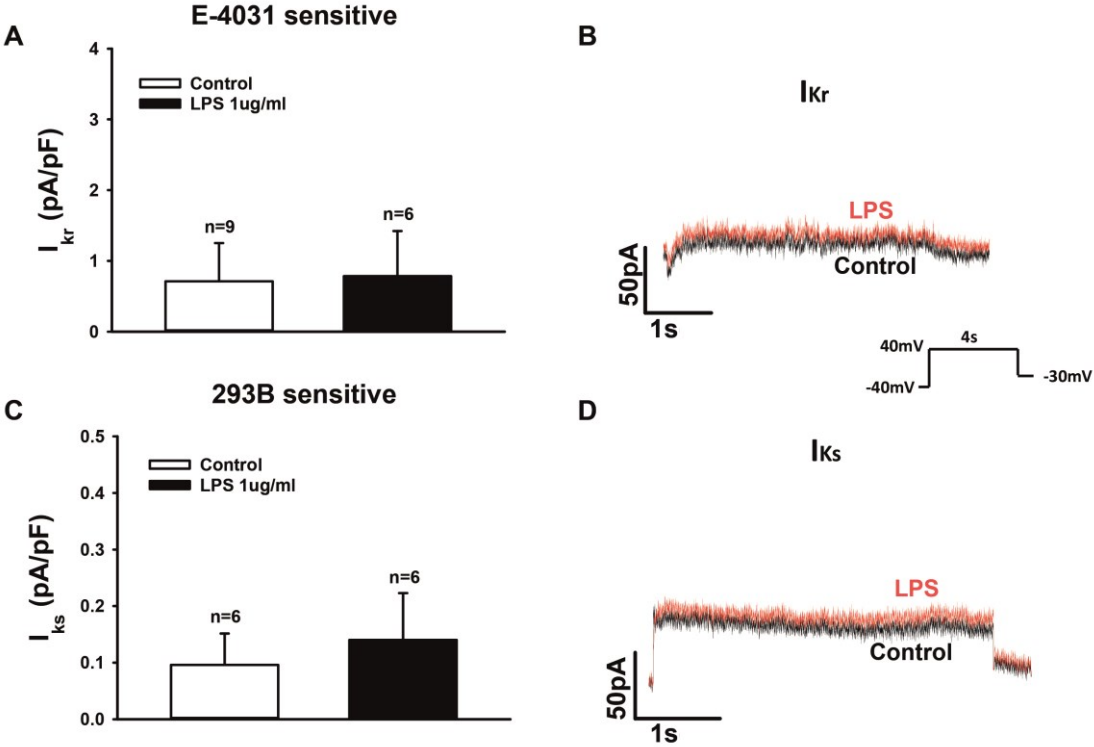


Figure S7

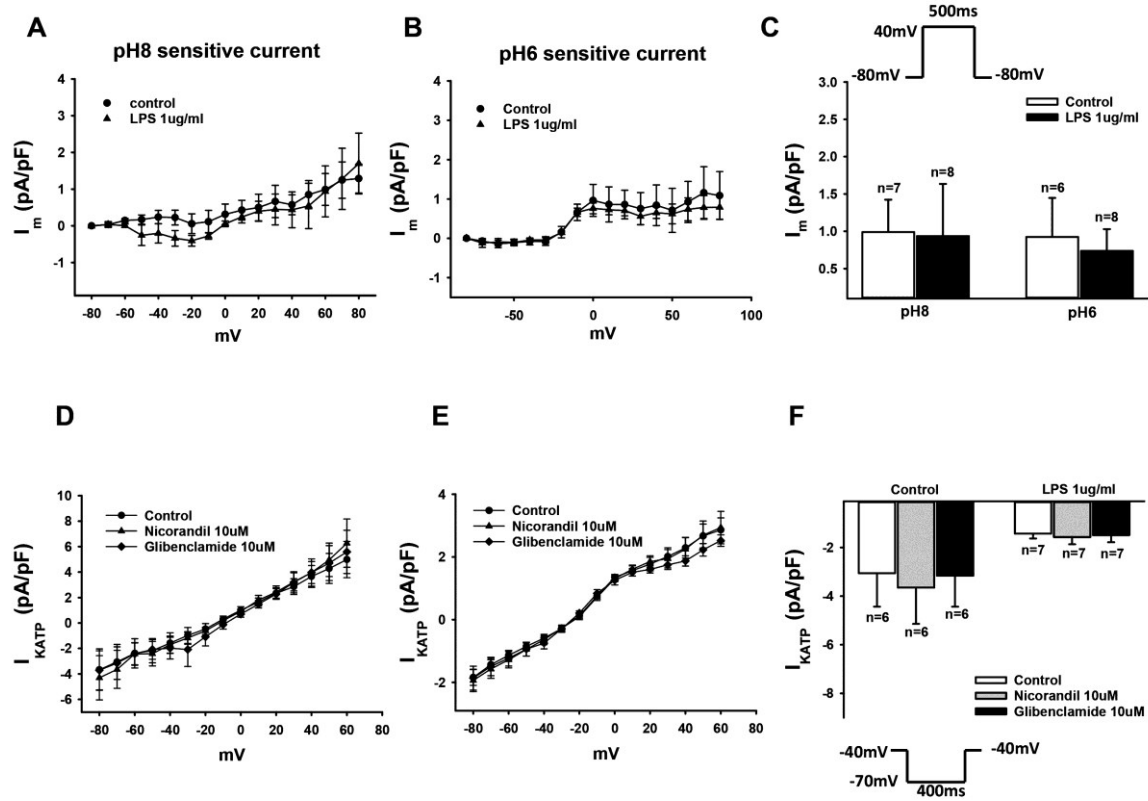


Figure S8

